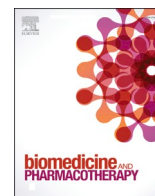




Since January 2020 Elsevier has created a COVID-19 resource centre with free information in English and Mandarin on the novel coronavirus COVID-19. The COVID-19 resource centre is hosted on Elsevier Connect, the company's public news and information website.

Elsevier hereby grants permission to make all its COVID-19-related research that is available on the COVID-19 resource centre - including this research content - immediately available in PubMed Central and other publicly funded repositories, such as the WHO COVID database with rights for unrestricted research re-use and analyses in any form or by any means with acknowledgement of the original source. These permissions are granted for free by Elsevier for as long as the COVID-19 resource centre remains active.



Oral IRAK4 inhibitor BAY-1834845 prevents acute respiratory distress syndrome

Qianqian Li, Rui Li, Hanlin Yin, Suli Wang, Bei Liu, Jun Li, Mi Zhou, Qingran Yan^{*}, Liangjing Lu^{*,1}

Department of Rheumatology, Renji Hospital, School of Medicine, Shanghai Jiao Tong University, 145 Middle Shandong Rd, Shanghai 200001, China

ARTICLE INFO

Keywords:

Acute respiratory distress syndrome
Cytokine release syndrome
IRAK4 inhibitor

ABSTRACT

Acute respiratory distress syndrome (ARDS) is a lethal clinical entity that has become an emergency event with the outbreak of COVID-19. However, to date, there are no well-proven pharmacotherapies except dexamethasone. This study is aimed to evaluate IRAK4 inhibitors as a potential treatment for ARDS-cytokine release syndrome (CRS). We applied two IRAK4 inhibitors, BAY-1834845 and PF-06650833 to an inhaled lipopolysaccharide (LPS)-induced ARDS mouse model with control of high dose dexamethasone (10 mg/kg). Unexpectedly, although both compounds had excellent IC₅₀ on IRAK4 kinase activity, only BAY-1834845 but not PF-06650833 or high dose dexamethasone could significantly prevent lung injury according to a blinded pathology scoring. Further, only BAY-1834845 and BAY-1834845 combined with dexamethasone could effectively improve the injury score of pre-existed ARDS. Compared with PF-06650833 and high dose dexamethasone, BAY-1834845 remarkably decreased inflammatory cells infiltrating lung tissue and neutrophil count in BALF. BAY-1834845, DEX, and the combination of the two agents could decrease BALF total T cells, monocyte, and macrophages. In further cell type enrichment analysis based on lung tissue RNA-seq, both BAY-1834845 and dexamethasone decreased signatures of inflammatory cells and effector lymphocytes. Interestingly, unlike the dexamethasone group, BAY-1834845 largely preserved the signatures of naïve lymphocytes and stromal cells such as endothelial cells, chondrocytes, and smooth muscle cells. Differential gene enrichment suggested that BAY-1834845 downregulated genes more efficiently than dexamethasone, especially TNF, IL-17, interferon, and Toll-like receptor signaling.

1. Introduction

Acute respiratory distress syndrome (ARDS) is a critical respiratory illness associated with infection, autoimmunity, and injuries. The overall mortality rate is as high as 30–40 % [1]. The main pathological features are extensive damage to the barriers of lung epithelial and endothelial cells, diffuse damage to lung capillaries, enhanced permeability, and the neutrophil influx into the lung tissue, resulting in multiple injuries to organ function leading to respiratory failure and high mortality [2–4].

Studies have shown that cytokine release syndrome (CRS) plays a vital role in ARDS [5,6]; CRS refers to the excessive and rapid production of proinflammatory cytokines by alveolar macrophages, including tumor necrosis factor- α (TNF- α), interleukin-6 (IL-6), interleukin-1 β (IL-1 β) and interferon (IFN)-induced chemokines that drive the

inflammatory response and promote a further influx of neutrophils and lymphocytes, resulting in overactivation of the immune system [7]. During the COVID-19 pandemic, ARDS-CRS was strongly associated with severe cases [8–11].

Previously, treatment for ARDS focused on lung-protective ventilation that reduced mortality [12]. No specific pharmacotherapies have been identified partially because multiple drug treatments, including inhalation or drip infusion of synthetic surfactants [13], intravenous endotoxin antibodies, ketoconazole, ibuprofen [14] and inhalation nitric oxide (iNO) [15], have proven to be ineffective. Since the COVID-19 pandemic, the increase in ARDS cases has spawned a series of investigations of anti-inflammatory drugs. Among these explorations, only dexamethasone showed benefits on mortality in severe COVID-19 pneumonia [16]. Other medicines, such as the JAK inhibitors tofacitinib and baricitinib, are beneficial to recovery, yet are basically for

^{*} Corresponding authors.

E-mail addresses: yanqingran@163.com (Q. Yan), lu_liangjing@163.com (L. Lu).

¹ ORCID: 0000-0001-9116-6038.

patients with the moderate disease who receive noninvasive ventilation [17,18], and the IL-6R blocker tocilizumab has failed to improve primary outcomes in COVID-19 patients [19]. Therefore, anti-inflammation is the only pharmaceutical strategy for ARDS that has been clinically proven thus far, although new candidate agents are still greatly needed.

Interleukin 1 receptor-associated kinase 4 (IRAK4) is a serine/threonine kinase that mediates innate immune and inflammatory responses [20]. It is an essential signal transducer downstream of the interleukin-1 receptor (IL-1R), interleukin-18 receptor (IL-18R), and Toll-like receptors 4 and 7–9 (TLR 4 and TLR 7–9) [21,22]. When binding with ligands, the intracellular domains of IL-1R/IL18R/TLRs typically recruit myeloid differentiation primary response 88 (MyD88) adaptor protein, IRAK4 and IRAK1 to form a complex myddosome [23–25], which activates IRAK4 autophosphorylation, followed by phosphorylation of IRAK1 and subsequent activation of NF- κ B, mitogen-activated protein kinase (MAPK) or interferon regulatory factor (IRF) signaling pathways [26–28], which produces proinflammatory cytokines, chemokines, and destructive enzymes, leading to inflammation and mediating innate immunity [29,30]. Genetically targeting IRAK4 has been shown to inhibit systemic inflammation powerfully. IRAK4-deficient animals are entirely resistant to a lethal dose of lipopolysaccharide (LPS) [29]. IRAK4-inactive knock-in mice were completely resistant to LPS- and CpG-induced shock [31]. Given that the cytokine activation pattern of COVID-CRS largely overlaps with the cytokines regulated by IRAK4, some researchers have speculated that IRAK4 is a potential treatment target for COVID-19 patients with systemic inflammation [32,33].

Recently, the theoretical druggability of IRAK4 has been put into practice. BAY-1834845 and PF-06650833 are two IRAK4 inhibitors [34, 35] that have published results from phase I clinical trials. This study aimed to investigate the potential efficacy of IRAK4 inhibitors in ARDS.

2. Method and materials

2.1. IC_{50} and IRAK4 kinase inhibition efficiency of BAY-1834845 and PF-06650833

The IC_{50} (semimaximum inhibitory concentration) values of BAY-1834845 and PF-06650833 were assessed by mobility shift assay (MSA). After the signal was measured, the inhibition rate of the compound at each concentration was calculated. Then nonlinear curve fitting was performed with the logarithmic concentration-inhibition rate to obtain the IC_{50} value of the compound.

2.2. ARDS mouse model

Modeling. Female Balb/c mice (aged 6–7 weeks) were purchased from Shanghai Sippe-Bk Lab Animal Co., Ltd. (China) and were housed in an SPF animal room for seven days to adapt to the environment. The mice were housed under a controlled temperature and humidity with a standard day-night cycle and free access to food and water. For modeling, 50 μ l PBS or LPS (700 μ g/ml, Sigma) was injected into the trachea of each mouse with a special atomized aerosol needle. All animal experiments were approved by the Animal Care Committee of Shanghai Jiao Tong University.

Drugs. All drugs were given orally, including BAY-1834845 (150 mg/kg, Medicilon), PF-06650833 (100 mg/kg, Medicilon), or dexamethasone (10 mg/kg). PBS (10 ml/kg) was used as vehicle control.

Treatments. For prevention, all drugs were given 30 min before LPS modeling. In regard to treatment, all mice received twice oral therapeutic agents 4 h and 12 h after LPS modeling.

2.3. Pathological assessment of mouse lung tissue

The lungs of the mice were harvested, fixed with formalin solution, embedded in paraffin, and cut into 5- μ m-thick slides. Three slices were

randomly picked up for each sample with a minimal interval of 20 μ m. Haematoxylin and eosin (HE) staining was applied to the slices. A pathologist blindly scored the lung tissue according to the Smith lung injury score [36]. Briefly, the severity of five parameters— inflammation, edema, hemorrhage, atelectasis, and formation of hyaline membrane—was scored on a 0- to 4-point scale: 0, no damage; 1, damaged visual field percentage \leq 25 %; 2, 25 % < damaged visual field percentage \leq 50 %; 3, 50 % < damaged visual field percentage \leq 75 %; and 4, diffuse injury. A total score for a field at 400x magnification (NIKON Eclipse Ci) was calculated by adding the scores of all five parameters. For the selection of the microscopic fields, each slice was divided into quadrants, then 3 non-overlapping fields were randomly pick-up in each quadrant for observation and scoring, and the average of the scores of twelve observation fields was taken as the score for one slice. Each sample contains three discontinuous slices at minimal 20 μ m intervals and the average of these three slides is the final score for each sample.

2.4. Broncho-alveolar lavage fluid (BALF) analysis

BALF was harvested from each mouse at 4 h and 24 h after LPS modeling. In brief, 0.5 ml PBS was used to wash the lung twice through a tracheal cannula. As much BALF was collected as possible and then centrifuged at 4 $^{\circ}$ C. Total cell counts and differential cell counts were quantified using an automatic blood cell analyzer (Mindray, BC-5000). According to the manufacturer's instructions, the secretion of IL-18, IL-6, and TNF- α in BALF was measured using enzyme-linked immunosorbent assay (ELISA) kits (Beyotime Biotechnology). The levels of lactate dehydrogenase (LDH) activity in the BALF were measured by an LDH Assay Kit (Abcam, ab102526) following the manufacturer's instructions.

2.5. Flow cytometry analysis of BALF

Cell suspensions were obtained from BALF and were washed and resuspended in PBS-1 %BSA before FACS analysis. All flow cytometry data was acquired using FACS Canto II (BD) and data was analyzed using FlowJo 10.4. The following antibodies were used in flow cytometric analyses: BV421 Hamster Anti-Mouse TCR β Chain (BD Horizon, catalog no. 562839), APC-CyTM7 Rat Anti-Mouse CD4 (BD Pharmingen, catalog no. 565650), APC Rat Anti-Mouse CD8 α (BD Pharmingen, catalog no. 553035), PE Mouse Anti-Mouse NK-1.1 (BD Pharmingen, catalog no. 557391), APC-CyTM7 Rat Anti-CD11b (BD Pharmingen, catalog no. 557657), FITC anti-mouse CD11c Antibody (Biolegend, catalog no. 117306), F4/80 Monoclonal Antibody APC (eBioscience, catalog no. 17-4801-80), PE Rat anti-Mouse CD14 (BD Pharmingen, catalog no. 553740), PE Rat Anti-Mouse Siglec-F (BD Pharmingen, catalog no. 552126).

2.6. RNA sequencing (RNA-seq) of lung tissue

Lung tissue RNA (RNA integrity number \geq 7) was extracted with the mirVana miRNA Isolation Kit (Ambion). RNA libraries were prepared with the TruSeq Stranded mRNA kit and sequenced by HiSeqTM 2500 (Illumina). RNA-seq fastq files were processed using bowtie2 [37] and xPpress [38]. Differentially expressed genes (DEGs) were identified using DESeq (2012) [39]. A P value < 0.05 and fold change > 2 or fold change < 0.5 were set as the threshold for significantly differential expression. Hierarchical cluster analysis of DEGs was performed to explore transcript expression patterns. Gene Ontology (GO) enrichment, Kyoto Encyclopedia of Genes and Genomes (KEGG) pathway enrichment analysis [40] and xCell analysis [41] were used to analyze the patterns of differential gene expression of different groups.

2.7. Cytokine expression using a Luminex panel

Peripheral blood mononuclear cells from healthy humans (hPBMC,

TPCS, PB010C) were incubated with different reagents (PBS/BAY-1834845/PF-06650833) for 20 h at a final concentration of 500nmol/L, then stimulated with LPS (0.1 ug/ml). After 5 h, the supernatant was collected and the release of 48 cytokines was detected using Luminex (X-200) according to the instructions of bioplex Pro Human Cytokine Screening Panel Kit (BiO-RAD, 12007283). Heatmap analysis was used to visualize the changes in 48 cytokines of different reagents.

2.8. Statistical analysis

The data conforming to a normal distribution are described as the mean and standard deviation ($M \pm SD$), and the or not working to a normal distribution are expressed as the median and interquartile range (IQR). Comparisons between two groups for data conforming to a normal distribution were performed with an unpaired t-test and ANOVA. The Mann-Whitney U test was used for nonparametric testing when comparing data between groups of semi-quantitative data or not conforming to a normal distribution. All data were analyzed using GraphPad Prism 8.0 (La Jolla, USA) and IBM SPSS Statistics 23.0 (IBM, USA), and $p < 0.05$ was considered indicative of a significant difference.

3. Result

3.1. In vitro inhibition of IRAK4 activity by BAY-1834845 and PF-06650833

BAY-1834845 contains an isoindazole as its core structure, while PF-06650833 is quite different and has isoquinoline as its core (Fig. 1A, B). However, although both compounds are very potent against IRAK4, PF-06650833 is several folds better [23,34,42]. We measured the kinase activity of IRAK4 in vitro in the presence of the two compounds and found that the IC_{50} values were 3.55 nM and 0.52 nM (Fig. 1C, D), consistent with previously published data. In an in vitro treatment of LPS stimulated human PBMC, both compounds decreased inflammatory cytokines secretion effectively, such as IL-1, IFN- γ , TNF- α , and IL-17 (Fig. 1E).

3.2. BAY-1834846 ameliorated lung injury in the LPS-induced ARDS model

To investigate whether IRAK4 inhibitors could work in ARDS, we induced acute lung injury with a single dose of intratracheal LPS. First,

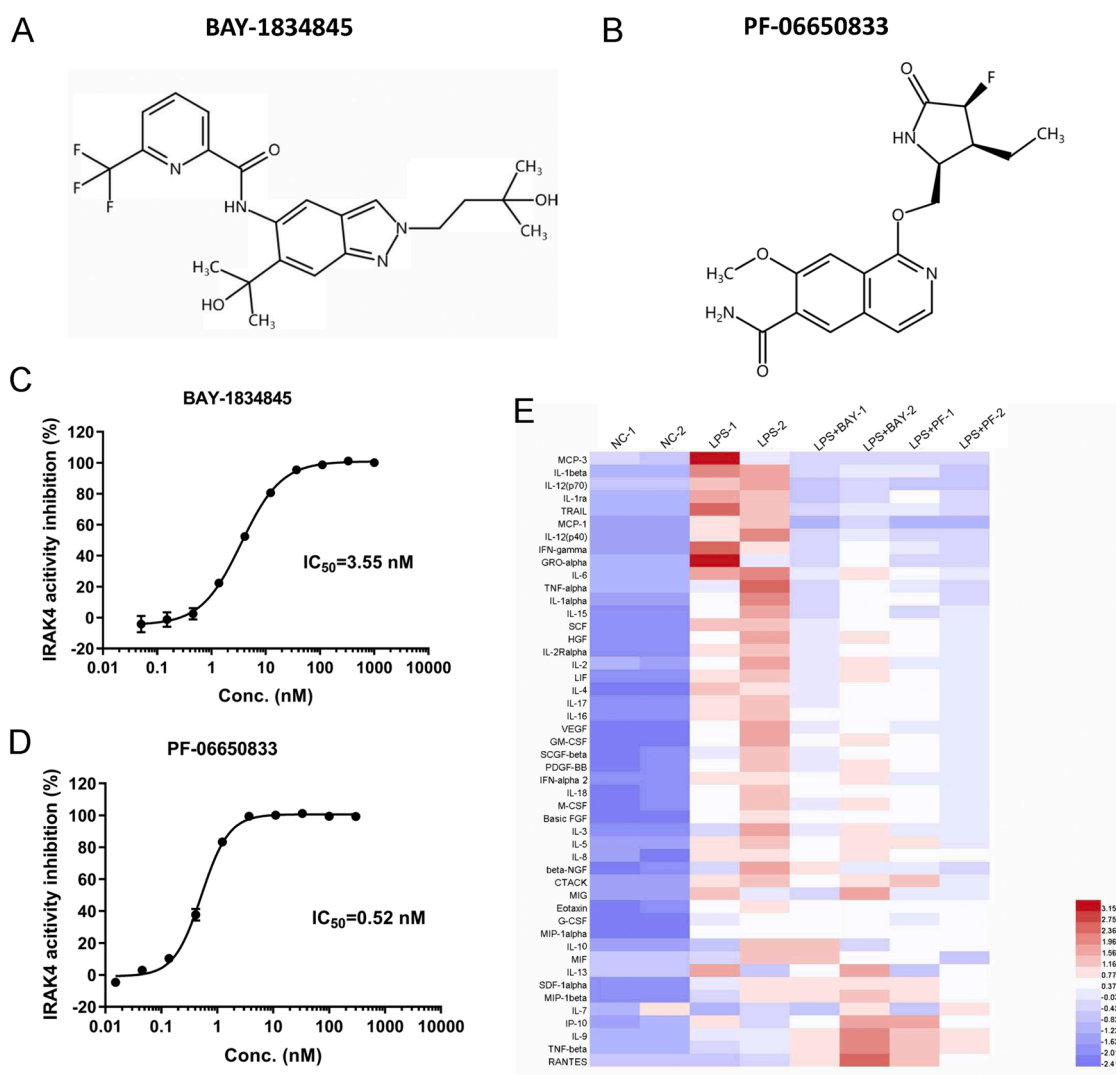


Fig. 1. IRAK4 IC_{50} calculation and in vitro effect on cytokine secretion by hPBMC of compounds BAY-1834845 and PF-06650833. (A and B) Chemical structures of BAY-1834845 and PF-06650833. BAY-1834845 contains an isoindazole as its core structure, while PF-06650833 is quite different and has isoquinoline as its core. (C and D) The IC_{50} values of BAY-1834845 and PF-06650833 were obtained by nonlinear curve fitting with a logarithmic concentration-inhibition rate. (E) Cytokine secretion of hPBMC upon BAY-1834845 or PF-06650833 treatment both in 500 nM. BAY: BAY-1834845; PF: PF-06650833.

the mice were briefly pre-treated with the IRAK4 inhibitors BAY-1834845 or PF-06650833 or with dexamethasone (DEX) as a positive control and received another dose for consolidation 6 h later (Fig. 2A). Twenty-four hours after LPS inhalation, alveolar cells were destroyed, the cytoplasm leaked out, interstitial edema and hemorrhage were evident, and a hyaline membrane was formed compared with the cells of the normal control group. All these pathological changes were attenuated in the BAY-1834845 group, as well as in the DEX group. However, in the PF-06650833 group, although the alveolar structure and

interstitial effusion were somewhat improved, neutrophil infiltration was not reduced (Fig. 2B). Histological scores integrating inflammation, edema, hemorrhage, atelectasis, and hyaline membrane, reflecting overall lung injury, unexpectedly showed statistically significant relief only in the BAY-1834845 group but not in the DEX group or PF-06650833 group (Fig. 2C), see more original images in Supplementary data (Supplementary Figs. 1–5). For each pathological dimension above, BAY-1834845 showed a robust and significant decrease in inflammation infiltration compared with DEX and PF-06650833 (Fig. 2D), while other

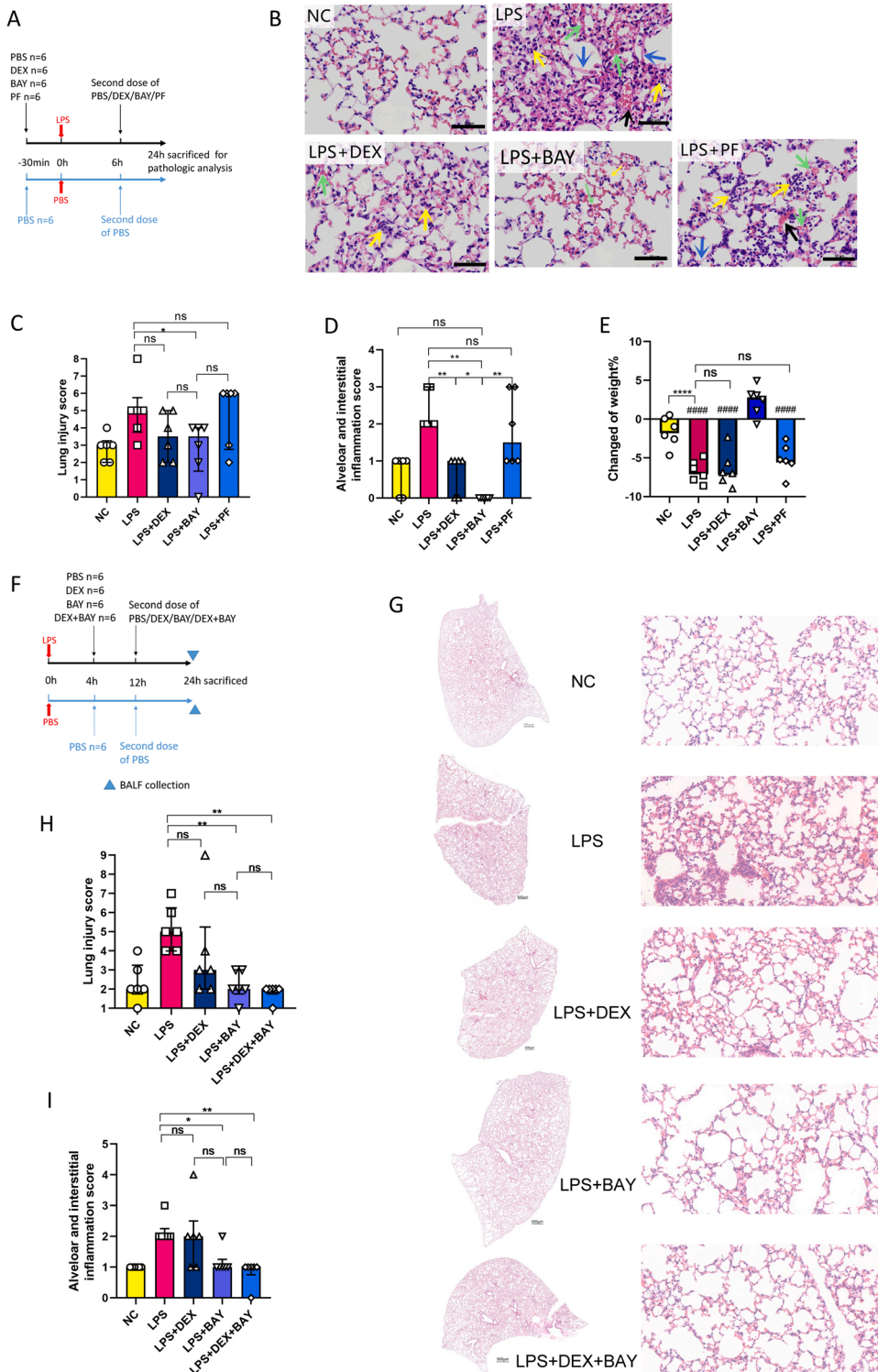


Fig. 2. BAY-1834845 effectively prevented lung injury in LPS-induced ARDS mice. (A) Prevention and modeling protocol. (B) Representative images of HE staining of lung tissue from of prevention model. Yellow arrows: neutrophil infiltrations around blood vessels and the alveolar cavity. Blue arrows: narrowed alveolar cavity and hyaline membrane formation. Green arrows: slight alveolar wall capillary congestion. Black arrows: mild congestion of capillaries of the alveolar wall. Bars, 50 μm. (C) Smith lung injury score of prevention model (median and IQR). (D) Alveolar and interstitial inflammation scores of prevention model (median and IQR). (E) Percentage change in body weight of prevention model. (F) Treatment protocol of pre-existed ARDS. (G) Representative images of HE staining of lung tissue of treatment model. Bars, 20 μm. (H) Smith lung injury score of each group in treatment model (median and IQR). (I) Alveolar and interstitial inflammation scores of treatment model (median and IQR). Fig C, D, H, and I: Mann–Whitney U test, Fig E: One-way ANOVA, # represents comparisons between the pointed and BAY-1834845 group; ##### p < 0.0001; * p < 0.05, ** p < 0.01, *** p < 0.001, **** p < 0.0001. ns: not statistically significant. BAY: BAY-1834845; PF: PF-06650833; DEX: dexamethasone.

dimensions were not statistically meaningful (Supplementary Fig 6). To assess the general state of mice, we additionally monitored the weight of each mouse. Although in merely one day, the mice receiving LPS lose near 10 % of body weight. DEX might help prevent inflammation but did not help counteract weight loss, while BAY-1834845 seemed interesting to neutralize the weight reduction (Fig. 2E).

Further, we treated pre-existed ARDS with BAY-1834845, DEX, and the combination of the two agents 4 h of post-modeling (Fig. 2F). All three treatments could reduce the interstitial inflammation, as well as

hemorrhage and hyaline membrane (Fig. 2G). However, when we calculated the pathological score, again, only BAY-1834845 and the combination therapy significantly decreased the overall pathological score (Fig. 2H) and interstitial inflammation score (Fig. 2I). Other dimensions such as hemorrhage and hyaline membrane are not statistically improved in any treatment groups (Supplementary Fig 7).

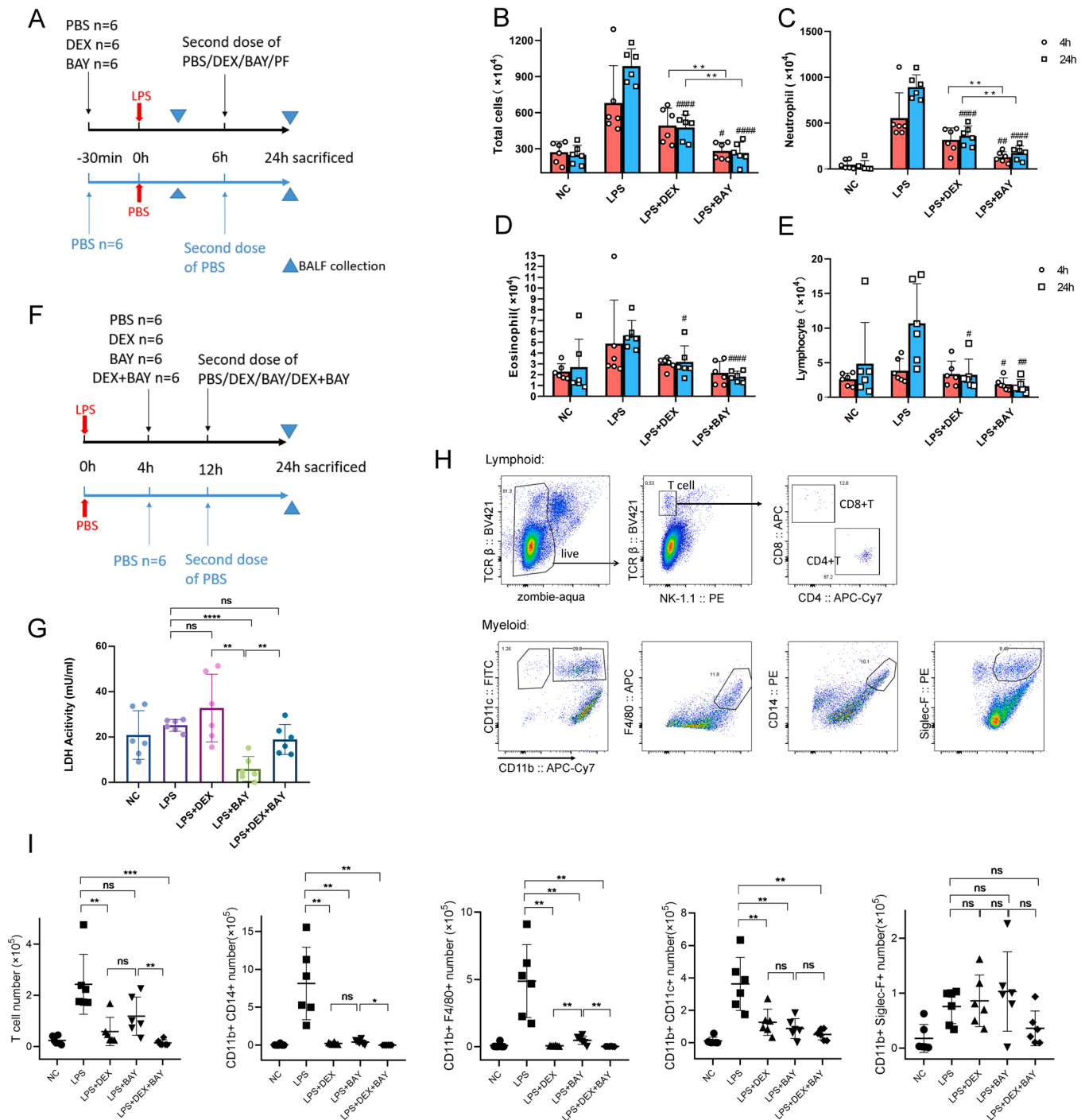


Fig. 3. Effect of BAY-183484 and dexamethasone in reducing inflammatory cells in BALF. (A) In the prevention model, BALF was collected 4 h and 24 h after modeling. (B-E) The counts of total cells, neutrophils, eosinophils, and lymphocytes in BALF. ANOVA, # represents comparison between the pointed group and LPS group; # $p < 0.05$, ## $p < 0.01$, ### $p < 0.001$. * $p < 0.05$; ** $p < 0.01$. (F) In the treatment model, BALF was collected 24 h after modeling. (G) LDH activity of BALF. (H and I) Flow cytometry of immune cells in BALF. Unpaired t-test, * $p < 0.05$; ** $p < 0.01$; *** $p < 0.001$; **** $p < 0.0001$. ns: not statistically significant. BALF: bronchoalveolar lavage fluid; BAY: BAY-1834845; DEX: dexamethasone.

3.3. BAY-1834845 reduced inflammatory cells in BALF

Based on the histological findings, we investigated the anti-inflammatory effects of BAY-1834845 through BALF cell counting (Fig. 3A). The numbers of cells with acute inflammation, including neutrophils and eosinophils, as well as the total cell number in BALF, began to increase rapidly 4 h after LPS modeling and continued to increase at 24 h. Lymphocyte counts increased in the later stage. Both

BAY-1834845 and DEX effectively reduced the numbers of all three types of inflammatory cells in BALF 24 h later. However, in the more acute phase at 4 h, only BAY-1834845 showed significant reductions in neutrophil, lymphocyte, and total cell counts. Unexpectedly, a direct comparison between BAY-1834845 and DEX showed that BAY-1834845 reduced the neutrophil count more effectively, which was consistent with the findings of lung histology above (Fig. 3B–E). In addition, DEX and BAY-1834845 showed some extent of reduction of BALF total

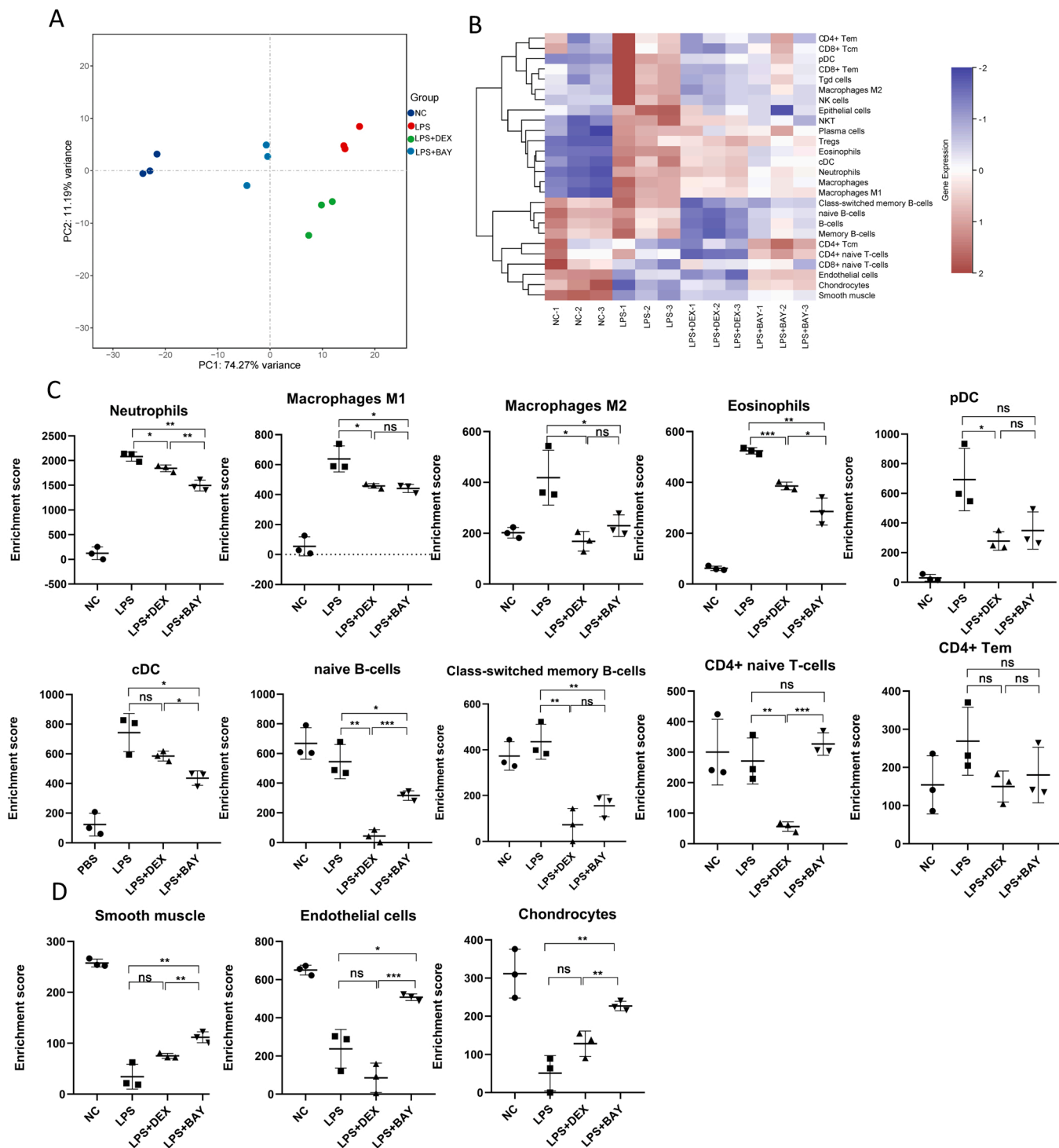


Fig. 4. BAY-1834845 decreased immune cell signatures while protecting stromal cell signatures on lung tissue RNA-seq. (A) PCA map between the four groups. (B) Heatmap of the enrichment score for 26 cell types by the xCells database. (C) Enrichment scores of representative immune cells of the lung. (D) Significantly changed enrichment scores of lung stromal cells. Unpaired t-test, * $p < 0.05$; ** $p < 0.01$; *** $p < 0.001$; ns: not statistically significant. BAY: BAY-1834845; DEX: dexamethasone.

protein, although no statistical significance was found possibly because of the large dispersion of the data (Supplementary Fig 8).

In the treatment model (Fig. 3F), BAY-1834845, DEX, and the combination of the two agents all reduced BALF LDH activity

significantly, while BAY-1834845 showed the most significant effect (Fig. 3G). In further flow cytometry analysis, all these three treatments could decrease total T cells, CD11b+CD14 + monocyte. Especially for total T cells, the combination therapy is superior to monotherapy. For

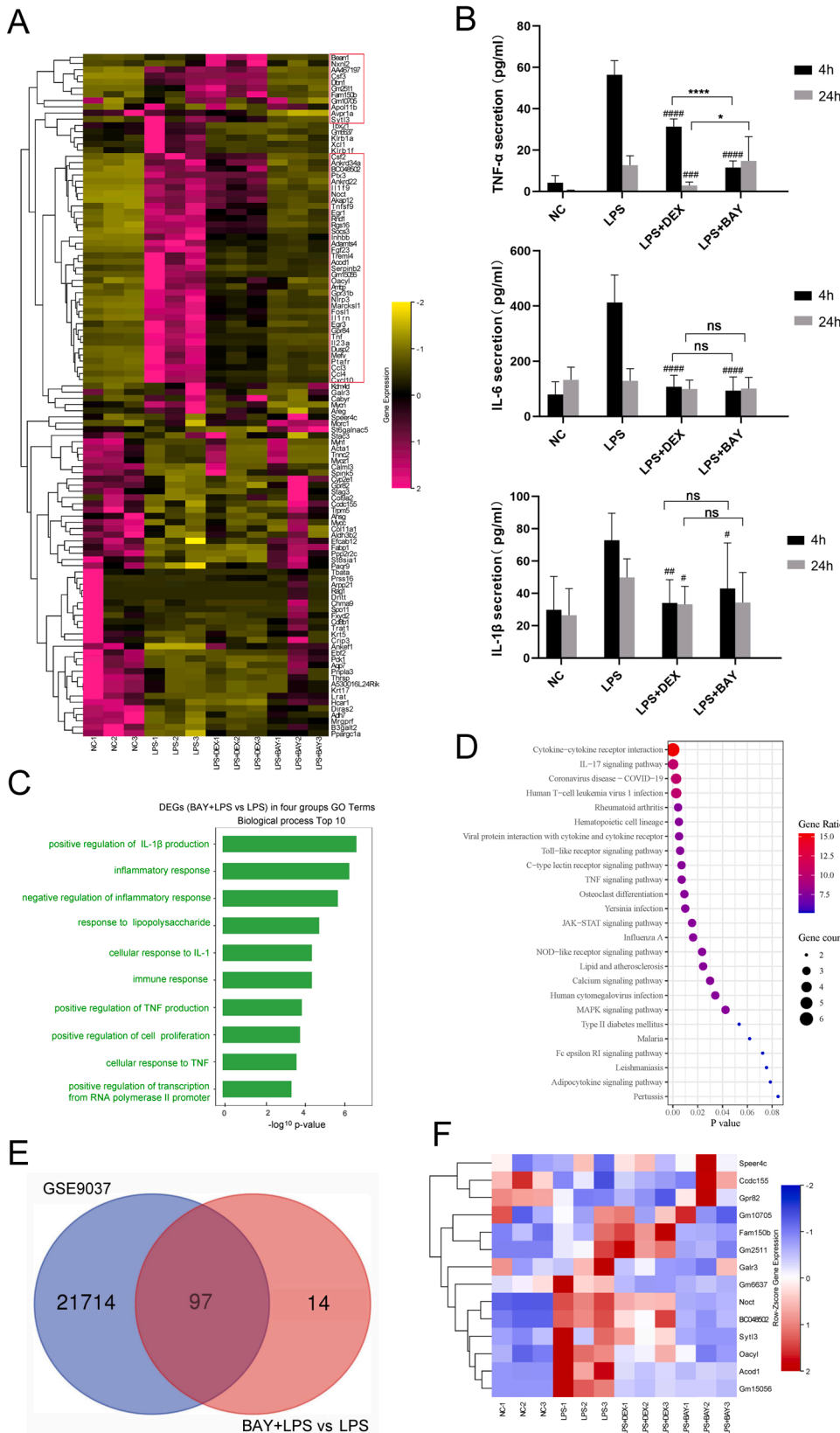


Fig. 5. BAY-1834845 regulated inflammation and innate immunity with minor potential off-target effects in ARDS lung tissue. (A) The heatmap of different genes (DEGs) between BAY-1834845 and LPS groups (P-value < 0.05 and fold change ≥ 2). Genes in the red box were not as effectively suppressed by dexamethasone as BAY-1834845. (B) The secretion of representative cytokines in BALF. # represents a comparison of pointed group with the LPS group; #p < 0.05, ##p < 0.01, ###p < 0.001, ####p < 0.0001. *p < 0.05, ***p < 0.0001, ns: not statistically significant, unpaired t-test. (C) The top 10 GO enrichment of DEGs from the red box in (A). (D) The KEGG pathway analysis of DEGs from the red box in Fig. 5A. (E) Venn diagram showed shared and unique parts between DGEs of GSE9037 and DEGs of BAY-1834845 vs LPS comparison. (F) Expressions of all fourteen DEGs of BAY-1834845 versus LPS groups that were not overlapped with GSE9037. BAY: BAY-1834845; DEX: dexamethasone. (For interpretation of the references to color in this figure legend, the reader is referred to the web version of this article.)

macrophages, both F4/80 + and CD11c+ marked populations could be decreased by all the three treatments. Siglec-F+ resident alveolar eosinophils were not significantly affected by the treatments (Fig. 3H and I).

3.4. BAY-1834845 decreased immune cell signatures while preserved stromal cell signatures through digital sorting based on lung tissue RNA-seq

To further identify the detailed cell types that BAY-1834845 could regulate, we used cell type signatures based on lung tissue RNA-seq, harvested 4 h after LPS modeling. Principal component analysis (PCA) plots showed significant and clear differences in the interaction between the four groups (Fig. 4A). The degree of individual dispersion within the components was small, indicating that the results were stable and reliable. We used xCells for digital sorting based on a total of 27,818 genes that showed significant differences in 26 cell types across the four groups (Fig. 4B). Both BAY-1834845 and DEX decreased the signatures of most innate immune cells, including neutrophils, M1 and M2 macrophages, eosinophils, and plasmacytoid dendritic cells (pDCs), and classic dendritic cells (cDCs). At the same time, BAY-1834845 was more effective than DEX in decreasing the signatures of neutrophils, eosinophils, and cDCs (Fig. 4C).

Regarding adaptive immune cells, both BAY-1834845 and DEX could downregulate the enrichment score of effector or memory cells (Fig. 4B, C). Interestingly, compared with DEX which decreased both naïve and effector cell signatures nonselectively, BAY-1834845 seemed to target memory lymphocytes specifically and preserve naïve B and naïve CD4 T cell signatures close to those of the normal control (Fig. 4C). In addition, BAY-1834845 showed similar preservation of lung stromal cells, including signatures of smooth muscle cells, chondrocytes, and endothelial cells (Fig. 4D).

3.5. BAY-1834845 regulated inflammation and innate immunity genes more efficiently than dexamethasone

We picked up a total of 111 DEGs upon BAY-1834845 treatment (P -value < 0.05 and fold change ≥ 2 , Fig. 5A, Supplementary Fig 9). GO, and KEGG enrichment identified these genes mainly on immune and inflammation responses such as IL-17, TNF, TLR, and NF- κ B signaling (Supplementary Fig 10A, B). DEX had similar DEG enrichment results with BAY-1834845 (Supplementary Fig 10C, D). As a validation, the secretion of representative cytokines in BALF, including TNF- α , IL-6, and IL-1 β , was decreased by both BAY-1834845 and DEX (Fig. 5B). We noticed 48 genes not as effectively suppressed by DEX as BAY-1834845 (Fig. 5A, red boxes). To our surprise, these 48 genes were highly concentrated in IL-17 signaling, COVID-19, rheumatoid arthritis, and Toll-like receptor signaling (Fig. 5C, D).

In addition, to identify possible off-target effects of BAY-1834845, we compared the DEGs of BAY-1834845 versus LPS in our study with data GSE9037, transcriptome data of monocytes from IRAK4 kinase-dead mice. We found that 97 out of 111 DEGs (87.3 %) overlapped with GSE9037, as only minor DEGs may be associated with off-target change (Fig. 5E). The left 14 genes not overlapping with GSE9037 seem to have no direct connection with IRAK4 according to known signaling, and their functions are scattered, such as spermatogenesis (speerc4 and ccdc155) [43], body-weight maintenance (gpr82) [44], and dietary lipid absorption (noct and oacyl) [45,46] (Fig. 5F). Therefore, they cannot be attributed to a definite off-target effect unless further evidence is present. More importantly, the change of these fourteen genes upon BAY-1834845 is close to normal controls, suggesting beneficial effects rather than unexpected side effects.

4. Discussion

ARDS is an emergency and lethal clinical entity [47], especially against the background of the COVID-19 outbreak. It is characterized by

excessive inflammation, the leading cause of death [48,49]. Unfortunately, the pharmaceutical treatment of ARDS was not well investigated until the pandemic, and only dexamethasone was identified as effective for both moderate and severe ARDS cases.

IRAK4 is downstream of all TLRs, except TLR3 [22]. To pharmaceutically target IRAK4, small-molecule IRAK4 inhibitors were designed almost a decade ago. These compounds can inhibit the inflammatory signal transduction induced by TLRs (including TLR4, TLR7, TLR8, and TLR9) in vitro and in vivo [50–52] and reduce gouty inflammation in uric acid peritonitis [51] and ischaemic inflammation in most nephrectomized rats [53]. Supported by this evidence, many pharmaceutical companies are vigorously developing potent and safe IRAK4 inhibitors for clinical diseases [23], which are represented by a series of preclinical models, including collagen-induced arthritis [42,51], gout [51], lupus [54,55], inflammatory dermatitis [51], and activated B cell-like (ABC) subtypes of diffuse large B cell lymphoma (DLBCL) [51]. Two major small-molecule IRAK4 inhibitors, BAY-1834845 and PF-06650833, have finished phase I clinical trials. In addition, PF-06650833 has shown efficacy in a phase II clinical trial in patients with rheumatoid arthritis (RA) who responded insufficiently to methotrexate (NCT02996500). Other ongoing clinical trials of these two compounds are for the treatment of RA (NCT04413617), psoriasis (NCT03493269), hidradenitis suppurativa (NCT04092452), and COVID-19 pneumonia (NCT04933799). The initiation of this trial supports our hypothesis that IRAK4 inhibitor may treat lung inflammation, although this trial NCT04933799 is focused on moderate-to-severe COVID-19 pneumonia (but not including the most critical patients with anticipated survival < 72 h), a population not largely overlapping with the ARDS population.

Our study is the first to compare the two compounds head-to-head in one animal model. To our surprise, the two compounds, BAY-1834845 and PF-06650833, seemed not equally effective on ARDS, as assessed by histological examination. BAY-1834845 exhibited a much more substantial reduction in lung inflammation, especially neutrophil infiltration, than PF-06650833. Given the equally excellent IC_{50} of the two compounds, we infer that pharmacokinetic characteristics might contribute to the different in vivo effects. The single-dose pharmacokinetics of PF-06650833 published by Pfizer showed quite a high clearance rate in rats of 56 ml/min/kg, leading to a $T_{1/2}$ of merely 0.6 h. For larger animals, the $T_{1/2}$ of dogs and monkeys was 1.1 h and 1.7 h, respectively. The oral bioavailability in rats is moderate (34–50 %), and the oral bioavailability in dogs and monkeys is low (41 % and 6.9 %) [42]. With these parameters, the therapeutic efficiency of PF-06650833 has driven concerns in a preclinical model: in a collagen-induced arthritis model, the arthritis score of the PF-06650833 group was inferior to that of the group treated with tofacitinib, a JAK inhibitor that has been approved for RA treatment for years [56]. As result, Pfizer has developed a modified release tablet to improve the pharmacokinetics of the compound in a recent RA trial (NCT02996500). On the other hand, the favorable pharmacokinetic profiling of BAY-1834845 in rats was identified by our group to have a lower clearance rate of 6.68 ml/min/kg, a longer $T_{1/2}$ of 3.09 h, and one hundred percent bioavailability, which is entirely consistent with its excellent efficacy with more than 80 % inhibition of cytokine release even at 16 h following induction by LPS in mice.

To our surprise, the in vivo therapeutic effect of BAY-1834845 is not only statically different from PF-06650833 but also from dexamethasone, the only medicine currently proven to be effective for the survival of ARDS patients [57]. We are fully aware of the limitation of the single-dose design of our experiment, which cannot demonstrate a definite superior effect of BAY-1834845. However, the dexamethasone (10 mg/kg once) we applied is a short-term pulse dose and is higher than typical amounts of ARDS [58]. According to the classic dose translation [59], 10 mg/kg equals approximately 50 mg of dexamethasone once in humans, while the common dose for ARDS in clinical trials is 6–20 mg daily [16,57]. For BAY-1834845 and PF-06650833, we applied the same dose as reported in patent documents by Bayer and Pfizer, respectively,

at which the two compounds have been verified to be fully effective. Besides, the results of fewer BALF inflammatory cell counts and specific inhibition of IL-17 signaling, COVID-19, rheumatoid arthritis, and Toll-like receptor signaling upon BAY-1834845 treatment are supportive of our histological findings. It would be interesting and informative to analyze more detailed immune cell phenotypes by flow cytometry in the future, particularly on lung macrophage and dendritic cells, with an up-to-date identification panel. [60].

In terms of safety, infection is a major concern. Although IRAK4 is widely involved in innate immunity and inflammation, susceptibility to bacterial, fungal, viral mycobacterial, or parasitic infections in adults was not increased. Children genetically lacking IRAK-4 are susceptible to certain purulent infections, including G+ purulent bacteria, such as *Streptococcus pneumoniae* and *Staphylococcus aureus* [29]; as these patients enter puberty, susceptibility to infection becomes increasingly rare, and there have been no reports of serious viral or parasitic infections [61–64] or infection-related deaths after the age of 8 [65]. In our study, BAY-1834845 preserved naïve lymphocyte signatures and stromal cell signatures of lung tissue. Such preservation may help this compound avoid some side effects such as impaired pathogen defense and delayed tissue repair, which are common in patients receiving steroids.

5. Conclusions

IRAK4 kinase inhibiting is a feasible approach to treating ARDS cascade and needs further investigation.

Funding

This work was supported by the National Natural Science Foundation of China [81974251], Shanghai Hospital Development Center, Joint Research of New Advanced Technology Project [SHDC12018106] and Shanghai Municipal Commission of Health and Family Planning [20204Y0088].

CRedit authorship contribution statement

Qianqian Li: Performing experiments, Date curation, Visualization, Writing – original draft. **Rui Li:** Writing - initial draft, Methodology. **Hanlin Yin:** Methodology, Data analysis. **Suli Wang:** Methodology, Visualization. **Bei Liu:** Formal analysis, Writing – original draft. **Jun Li:** Methodology. **Mi Zhou:** Date curation, Visualization. **Qingran Yan:** Conceptualization, Validation, Methodology, Writing - initial draft. **Liangjing Lu:** Supervision, Conceptualization, Resources, Funding acquisition, Writing – review & editing, Project administration.

Conflict of interest statement

The authors declare that they have no conflicts of interest.

Availability of data and materials

The datasets used and/or analyzed during the current study are available from the corresponding author on reasonable request.

Acknowledgements

Thanks for the technical support provided by Shanghai Leadingtac Pharmaceutical Co., LTD.

Appendix A. Supporting information

Supplementary data associated with this article can be found in the online version at [doi:10.1016/j.biopha.2022.113459](https://doi.org/10.1016/j.biopha.2022.113459).

References

- [1] A. Salim, M. Martin, C. Constantinou, B. Sangthong, C. Brown, G. Kasotakis, et al., Acute respiratory distress syndrome in the trauma intensive care unit: morbid but not mortal, *Arch. Surg.* 141 (7) (2006) 655–658.
- [2] M.A. Matthay, L.B. Ware, G.A. Zimmerman, The acute respiratory distress syndrome, *J. Clin. Invest.* 122 (8) (2012) 2731–2740.
- [3] G.D. Rubenfeld, E. Caldwell, E. Peabody, J. Weaver, D.P. Martin, M. Neff, et al., Incidence and outcomes of acute lung injury, *N. Engl. J. Med.* 353 (16) (2005) 1685–1693.
- [4] M. Mora-Rillo, M. Arsuaga, G. Ramírez-Olivencia, F. de la Calle, A.M. Borobia, P. Sánchez-Secco, et al., Acute respiratory distress syndrome after convalescent plasma use: treatment of a patient with Ebola virus disease contracted in Madrid, Spain, *Lancet Respir. Med.* 3 (7) (2015) 554–562.
- [5] X. Zhao, R. Andersson, X. Wang, M. Dib, X. Wang, Acute pancreatitis-associated lung injury: pathophysiological mechanisms and potential future therapies, *Scand. J. Gastroenterol.* 37 (12) (2002) 1351–1358.
- [6] B.T. Thompson, R.C. Chambers, K.D. Liu, Acute respiratory distress syndrome, *N. Engl. J. Med.* 377 (6) (2017) 562–572.
- [7] H. Gerlach, Agents to reduce cytokine storm, *F1000Research* 5 (2016) 2909.
- [8] P. Weiss, D.R. Murdoch, Clinical course and mortality risk of severe COVID-19, *Lancet* 395 (10229) (2020) 1014–1015.
- [9] M.J. Cummings, M.R. Baldwin, D. Abrams, S.D. Jacobson, B.J. Meyer, E. M. Balough, et al., Epidemiology, clinical course, and outcomes of critically ill adults with COVID-19 in New York City: a prospective cohort study, *Lancet* 395 (10239) (2020) 1763–1770.
- [10] J.B. Moore, C.H. June, Cytokine release syndrome in severe COVID-19, *Science* 368 (6490) (2020) 473–474.
- [11] R. Channappanavar, S. Perlman, Pathogenic human coronavirus infections: causes and consequences of cytokine storm and immunopathology, *Semin. Immunopathol.* 39 (5) (2017) 529–539.
- [12] M.A. Matthay, D.F. McAuley, L.B. Ware, Clinical trials in acute respiratory distress syndrome: challenges and opportunities, *Lancet Respir. Med.* 5 (6) (2017) 524–534.
- [13] M. Chen, J. Lu, Q. Chen, L. Cheng, Y. Geng, H. Jiang, et al., [Statin in the treatment of ALI/ARDS: a systematic review and Meta-analysis based on international databases], *Zhonghua wei zhong Bing. ji jiu yi xue* 29 (1) (2017) 51–56.
- [14] G.R. Bernard, A.P. Wheeler, J.A. Russell, R. Schein, W.R. Summer, K.P. Steinberg, et al., The effects of ibuprofen on the physiology and survival of patients with sepsis. The Ibuprofen in Sepsis Study Group, *N. Engl. J. Med.* 336 (13) (1997) 912–918.
- [15] A. Afshari, J. Brok, A.M. Møller, J. Wetterslev, Inhaled nitric oxide for acute respiratory distress syndrome (ARDS) and acute lung injury in children and adults, *Cochrane Database Syst. Rev.* (7) (2010), Cd002787.
- [16] P. Horby, W.S. Lim, J.R. Emberson, M. Mafham, J.L. Bell, L. Linsell, et al., Dexamethasone in hospitalized patients with Covid-19, *N. Engl. J. Med.* 384 (8) (2021) 693–704.
- [17] P.O. Guimarães, D. Quirk, R.H. Furtado, L.N. Maia, J.F. Saraiva, M.O. Antunes, et al., Tofacitinib in patients hospitalized with Covid-19 pneumonia, *N. Engl. J. Med.* 385 (5) (2021) 406–415.
- [18] A.C. Kalil, T.F. Patterson, A.K. Mehta, K.M. Tomashek, C.R. Wolfe, V. Ghazaryan, et al., Baricitinib plus remdesivir for hospitalized adults with Covid-19, *N. Engl. J. Med.* 384 (9) (2021) 795–807.
- [19] J.H. Stone, M.J. Frigault, N.J. Serling-Boyd, A.D. Fernandes, L. Harvey, A. S. Foulkes, et al., Efficacy of tocilizumab in patients hospitalized with Covid-19, *N. Engl. J. Med.* 383 (24) (2020) 2333–2344.
- [20] S. Flannery, A.G. Bowie, The interleukin-1 receptor-associated kinases: critical regulators of innate immune signalling, *Biochem. Pharmacol.* 80 (12) (2010) 1981–1991.
- [21] S. Li, A. Strelow, E.J. Fontana, H. Wesche, IRAK-4: a novel member of the IRAK family with the properties of an IRAK-kinase, *Proc. Natl. Acad. Sci. USA* 99 (8) (2002) 5567–5572.
- [22] L.A. O'Neill, The interleukin-1 receptor/Toll-like receptor superfamily: 10 years of progress, *Immunol. Rev.* 226 (2008) 10–18.
- [23] W.T. McElroy, Interleukin-1 receptor-associated kinase 4 (IRAK4) inhibitors: an updated patent review (2016–2018), *Expert Opin. Ther. Pat.* 29 (4) (2019) 243–259.
- [24] G.M. Barton, R. Medzhitov, Toll-like receptor signaling pathways, *Science* 300 (5625) (2003) 1524–1525.
- [25] S.C. Lin, Y.C. Lo, H. Wu, Helical assembly in the MyD88-IRAK4-IRAK2 complex in TLR/IL-1R signalling, *Nature* 465 (7300) (2010) 885–890.
- [26] Z. Cao, J. Xiong, M. Takeuchi, T. Kurama, D.V. Goeddel, TRAF6 is a signal transducer for interleukin-1, *Nature* 383 (6599) (1996) 443–446.
- [27] R. Ferrao, H. Zhou, Y. Shan, Q. Liu, Q. Li, D.E. Shaw, et al., IRAK4 dimerization and trans-autophosphorylation are induced by Myddosome assembly, *Mol. Cell* 55 (6) (2014) 891–903.
- [28] Y. Qian, M. Commane, J. Ninomiya-Tsuji, K. Matsumoto, X. Li, IRAK-mediated translocation of TRAF6 and TAB2 in the interleukin-1-induced activation of NFκB, *J. Biol. Chem.* 276 (45) (2001) 41661–41667.
- [29] N. Suzuki, S. Suzuki, G.S. Duncan, D.G. Millar, T. Wada, C. Mirtsos, et al., Severe impairment of interleukin-1 and Toll-like receptor signalling in mice lacking IRAK-4, *Nature* 416 (6882) (2002) 750–756.
- [30] Z. Wang, H. Wesche, T. Stevens, N. Walker, W.C. Yeh, IRAK-4 inhibitors for inflammation, *Curr. Top. Med. Chem.* 9 (8) (2009) 724–737.

- [31] T.W. Kim, K. Staschke, K. Bulek, J. Yao, K. Peters, K.H. Oh, et al., A critical role for IRAK4 kinase activity in Toll-like receptor-mediated innate immunity, *J. Exp. Med.* 204 (5) (2007) 1025–1036.
- [32] N. Stoy, Involvement of interleukin-1 receptor-associated kinase 4 and interferon regulatory factor 5 in the immunopathogenesis of SARS-CoV-2 infection: implications for the treatment of COVID-19, *Front. Immunol.* 12 (738) (2021).
- [33] A. Gupta, H.J. Chun, Interleukin-1 receptor kinase 4 inhibition: achieving immunomodulatory synergy to mitigate the impact of COVID-19, *Front. Immunol.* 12 (2483) (2021).
- [34] M.D. Wiese, A.T. Manning-Bennett, A.Y. Abuhelwa, Investigational IRAK-4 inhibitors for the treatment of rheumatoid arthritis, *Expert Opin. Investig. Drugs* 29 (5) (2020) 475–482.
- [35] K.L. Lee, C.M. Ambler, D.R. Anderson, B.P. Boscoe, A.G. Bree, J.I. Brodfuehrer, et al., Discovery of clinical candidate 1-((2S,3S,4S)-3-ethyl-4-fluoro-5-oxopyrrolidin-2-yl)methoxy)-7-methoxyisoquinoline-6-carboxamide (PF-06650833), a potent, selective inhibitor of interleukin-1 receptor associated kinase 4 (IRAK4), by fragment-based drug design, *J. Med. Chem.* 60 (13) (2017) 5521–5542.
- [36] K.M. Smith, J.D. Mrozek, S.C. Simonton, D.R. Bing, P.A. Meyers, J.E. Connett, et al., Prolonged partial liquid ventilation using conventional and high-frequency ventilatory techniques: gas exchange and lung pathology in an animal model of respiratory distress syndrome, *Crit. Care Med.* 25 (25) (1997) 1888–1897.
- [37] B. Langmead, S.L. Salzberg, Fast gapped-read alignment with Bowtie 2, *Nat. Methods* 9 (4) (2012) 357–359.
- [38] A. Roberts, L. Pachter, Streaming fragment assignment for real-time analysis of sequencing experiments, *Nat. Methods* 10 (1) (2013) 71–73.
- [39] Anders S., Huber W. *Differential Expression of RNA-Seq Data at the Gene Level – the DESeq package.* *embl.*
- [40] M. Kanehisa, M. Araki, S. Goto, M. Hattori, M. Hirakawa, M. Itoh, et al., KEGG for linking genomes to life and the environment, *Nucleic Acids Res.* 36 (Database issue) (2008) D480–D484.
- [41] D. Aran, Z. Hu, A.J. Butte, xCell: digitally portraying the tissue cellular heterogeneity landscape, *Genome Biol.* 18 (1) (2017) 220.
- [42] K.L. Lee, Discovery of clinical candidate 1-((2S,3S,4S)-3-ethyl-4-fluoro-5-oxopyrrolidin-2-yl)methoxy)-7-methoxyisoquinoline-6-carboxamide (PF-06650833), a potent, selective inhibitor of interleukin-1 receptor associated kinase 4 (IRAK4), by fragment-based drug design 60 (13) (2017) 5521–5542.
- [43] K.A. Fakhro, H. Elbardisi, M. Arafa, A. Robay, J.L. Rodriguez-Flores, A. Al-Shakaki, et al., Point-of-care whole-exome sequencing of idiopathic male infertility, *Genet. Med.* 20 (11) (2018) 1365–1373.
- [44] K.M. Engel, K. Schröck, D. Teupser, L.M. Holdt, A. Tönjes, M. Kern, et al., Reduced food intake and body weight in mice deficient for the G protein-coupled receptor GPR82, *PLoS One* 6 (12) (2011), e29400.
- [45] N. Douris, S. Kojima, X. Pan, A.F. Lerch-Gaggl, S.Q. Duong, M.M. Hussain, et al., Nocturnin regulates circadian trafficking of dietary lipid in intestinal enterocytes, *Curr. Biol.* 21 (16) (2011) 1347–1355.
- [46] L. Wang, H. Qian, Y. Nian, Y. Han, Z. Ren, H. Zhang, et al., Structure and mechanism of human diacylglycerol O-acyltransferase 1, *Nature* 581 (7808) (2020) 329–332.
- [47] J.C. Densmore, P.R. Signorino, J. Ou, O.A. Hatoum, J.J. Rowe, Y. Shi, et al., Endothelium-derived microparticles induce endothelial dysfunction and acute lung injury, *Shock* 26 (5) (2006) 464–471.
- [48] J.Y. Chien, P.R. Hsueh, W.C. Cheng, C.J. Yu, P.C. Yang, Temporal changes in cytokine/chemokine profiles and pulmonary involvement in severe acute respiratory syndrome, *Respirology* 11 (6) (2006) 715–722.
- [49] P. Conti, G. Ronconi, A. Caraffa, C.E. Gallenga, R. Ross, I. Frydas, et al., Induction of pro-inflammatory cytokines (IL-1 and IL-6) and lung inflammation by Coronavirus-19 (COVI-19 or SARS-CoV-2): anti-inflammatory strategies, *J. Biol. Regul. Homeost. Agents* 34 (2) (2020) 327–331.
- [50] L.N. Tumey, D.H. Boschelli, N. Bhagirath, J. Shim, E.A. Murphy, D. Goodwin, et al., Identification and optimization of indolo[2,3-c]quinoline inhibitors of IRAK4, *Bioorg. Med. Chem. Lett.* 24 (9) (2014) 2066–2072.
- [51] P.N. Kelly, D.L. Romero, Y. Yang, A.L. Shaffer 3rd, D. Chaudhary, S. Robinson, et al., Selective interleukin-1 receptor-associated kinase 4 inhibitors for the treatment of autoimmune disorders and lymphoid malignancy, *J. Exp. Med.* 212 (13) (2015) 2189–2201.
- [52] A.A. Zarrin, K. Bao, Kinase inhibition in autoimmunity and inflammation, *Nat. Rev. Drug Discov.* 20 (1) (2021) 39–63.
- [53] M. Kondo, A. Tahara, K. Hayashi, M. Abe, H. Inami, T. Ishikawa, et al., Renoprotective effects of novel interleukin-1 receptor-associated kinase 4 inhibitor AS2444697 through anti-inflammatory action in 5/6 nephrectomized rats, *Naunyn Schmiede's Arch. Pharmacol.* 387 (10) (2014) 909–919.
- [54] S. Dudhgaonkar, S. Ranade, Selective IRAK4 inhibition attenuates disease in murine lupus models and demonstrates steroid sparing activity 198 (3) (2017) 1308–1319.
- [55] A.A. Corzo, E. Varfolomeev, The kinase IRAK4 promotes endosomal TLR and immune complex signaling in B cells and plasmacytoid dendritic cells, *Sci. Signal.* 13 (634) (2020).
- [56] A. Winkler, W. Sun, S. De, A. Jiao, M.N. Sharif, P.T. Symanowicz, et al., The interleukin-1 receptor-associated kinase 4 inhibitor PF-06650833 blocks inflammation in preclinical models of rheumatic disease and in humans enrolled in a Randomized Clinical Trial, *Arthritis Rheumatol.* 73 (12) (2021) 2206–2218.
- [57] J. Villar, C. Ferrando, D. Martínez, A. Ambrós, T. Muñoz, J.A. Soler, et al., Dexamethasone treatment for the acute respiratory distress syndrome: a multicentre, randomised controlled trial, *Lancet Respir. Med.* 8 (3) (2020) 267–276.
- [58] N.O. Al-Harbi, F. Imam, M.M. Al-Harbi, M.A. Ansari, K.M.A. Zoheir, H.M. Korashy, et al., Dexamethasone attenuates LPS-induced acute lung injury through inhibition of NF- κ B, COX-2, and pro-inflammatory mediators, *Immunol. Investig.* 45 (4) (2016) 349–369.
- [59] S. Reagan-Shaw, M. Nihal, N. Ahmad, Dose translation from animal to human studies revisited, *FASEB J.* 22 (3) (2008) 659–661.
- [60] Y. Fu, J. Wang, B. Zhou, A. Pajulas, H. Gao, B. Ramdas, et al., An IL-9-pulmonary macrophage axis defines the allergic lung inflammatory environment, *Sci. Immunol.* 7 (68) (2022) eabi9768.
- [61] C.L. Ku, H. von Bernuth, C. Picard, S.Y. Zhang, H.H. Chang, K. Yang, et al., Selective predisposition to bacterial infections in IRAK-4-deficient children: IRAK-4-dependent TLRs are otherwise redundant in protective immunity, *J. Exp. Med.* 204 (10) (2007) 2407–2422.
- [62] K. Yang, A. Puel, S. Zhang, C. Eidenschenck, C.L. Ku, A. Casrouge, et al., Human TLR-7-, -8-, and -9-mediated induction of IFN- α /beta and -lambda Is IRAK-4 dependent and redundant for protective immunity to viruses, *Immunity* 23 (5) (2005) 465–478.
- [63] C. Picard, H. von Bernuth, P. Ghandil, M. Chrabieh, O. Levy, P.D. Arkwright, et al., Clinical features and outcome of patients with IRAK-4 and MyD88 deficiency, *Medicine* 89 (6) (2010) 403–425.
- [64] H. von Bernuth, C. Picard, A. Puel, J.L. Casanova, Experimental and natural infections in MyD88- and IRAK-4-deficient mice and humans, *Eur. J. Immunol.* 42 (12) (2012) 3126–3135.
- [65] C. Picard, A. Puel, M. Bonnet, C.L. Ku, J. Bustamante, K. Yang, et al., Pyogenic bacterial infections in humans with IRAK-4 deficiency, *Science* 299 (5615) (2003) 2076–2079.